We are IntechOpen,
the world's leading publisher of
Open Access books
Built by scientists, for scientists

4,800
Open access books available

122,000
International authors and editors

135M
Downloads

Our authors are among the

154
Countries delivered to

TOP 1%
most cited scientists

12.2%
Contributors from top 500 universities

WEB OF SCIENCE™

Selection of our books indexed in the Book Citation Index
in Web of Science™ Core Collection (BKCI)

Interested in publishing with us?
Contact book.department@intechopen.com

Numbers displayed above are based on latest data collected.
For more information visit www.intechopen.com

Recognition of Contact State of Four Layers Arrayed Type Tactile Sensor by Using Neural Networks

Seiji Aoyagi
Kansai University
Japan

1. Introduction

An advanced tactile sensor is desired for the purpose of realizing complicated assembly tasks, recognizing objects in the space where vision sensor cannot be used (in the darkness, etc.), and so on. For example, development of a robot hand is important for realizing a practical humanoid robot. In this hand, a tactile sensor of micro size is desired to be developed to give a vivid sense of touch like a human being. There are two subjects in developing such sensor: one is fabrication of a practical sensor having numerous force sensing elements, and another is information processing of data obtained from these elements.

The human skin contains numerous force-sensing receptors distributed horizontally and vertically at intervals of about 1 mm (Maeno, 2000). Many artificial tactile sensors are proposed (Kinoshita, 1981; Lee & Nicholls, 1999; Shinoda, 2000; Ishikawa & Shimojo, 1988): however, none among them approaches the human equivalent because it is technically difficult to fabricate a sensor having numerous force sensing elements. To overcome this problem, several researches are carried out, which obtain and analyze stress distribution optically (Kamiyama et al., 2003; Hiraishi et al., 1989; Maekawa et al., 1994). However, it is still desirable to detect the stress distribution by setting many sensing elements and obtaining electrical signals from these elements like the human tactile sensing mechanism, which directly processes stress data from receptors (i.e., does not indirectly process once optically transformed data). This direct processing method would be preferable in the industrial viewpoint of sensing accuracy, and moreover in the academic viewpoint of human mimetics.

Micromachining based on semiconductor manufacturing is being widely researched (Kovacs, 1998). Numerous arrayed miniature force sensors with uniform performance are fabricated on a silicon wafer with fine resolution of several microns, which may make it possible to fabricate a practical tactile sensor. Tactile sensors proposed and developed based on micromachining are classified to piezoresistive (Kobayashi & Sagisawa, 1991; Ohka et al., 1990; Horie et al., 1995; Nguyen et al., 2004; Takao et al., 2005) and capacitive (Esashi et al., 1990; Kane et al., 2000; Suzuki et al., 1990; Lee et al., 2006). In dynamic measurement, piezoelectric type is also applicable (Yagi, 1991; Matsushita et al., 2004). Author is

fabricating a multiaxis piezoresistive type tactile sensor (Maeda et al., 2004; Izutani et al., 2004; Aoyagi et al., 2005) and a flexible tactile sensor of arrayed capacitive type (Aoyagi & Tanaka, 2007; Ono et al., 2008), which are described in the next section in detail.

Table 1 shows the comparison of characteristics of these sensors. The capacitive type has characteristics of nonlinear output, easy fabrication, and excellent sensitivity. The piezoelectric type has characteristics of acting also as an actuator, not applicable for the static sensing because of charge dissipation as time elapse. The piezoresistive type has characteristics of a linear output, and a wide range of strain detection.

	Capacitive	Piezoresistive	Piezoelectric
Detecting range	Narrow	Wide	Narrow
Sensitivity	Good	Normal	Normal
Power consumption	Small	Large	Small
Temperature dependence	Small	Big	Small
Digital procesing	Pulse	A/D converter necessary	A/D converter necessary
Linearity	Bad	Good	Good
CMOS compatible	Good	Good	Bad
Fabrication cost	Low	High	High
Sensing area	Small	Large	Small

Table 1. Comparison between characteristics of micromachined sensor types

In the reported micromachined tactile sensors, the force sensing elements are distributed two dimensionally on a surface. However, in the human skin, four kinds of tactile receptors (Meissner corpuscle, Merkel cell, Ruffini ending, and Pacinian corpuscle) are distributed three dimensionally, i.e., not only on the skin surface but also in the four corresponding depths of the skin (Maeno, 2000) (Fig. 1).
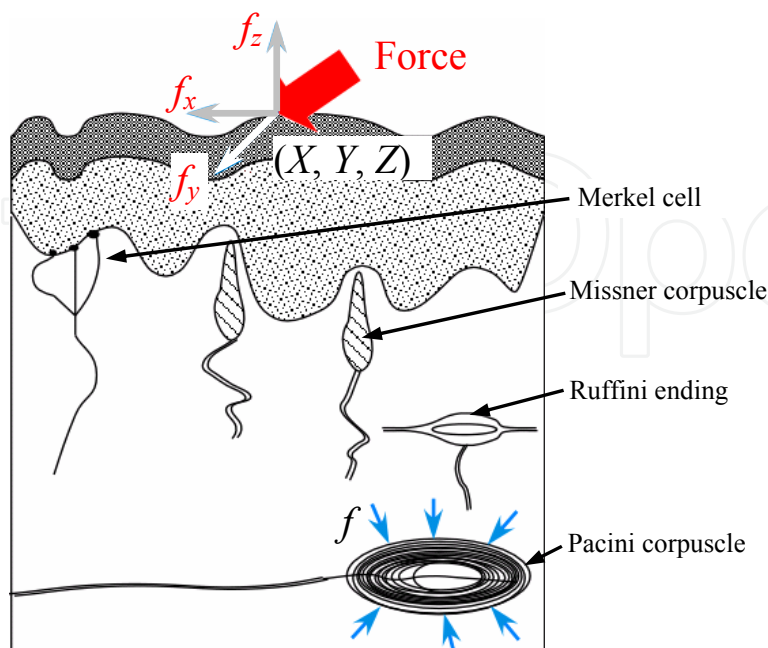

Fig. 1. Schematic view of human tactile receptors

In the human tactile sensing, the brain synthesizes nerve signals from many receptors and obtains cutaneous stress distribution to finally recognize the contact state. This human information processing mechanism has not been cleared yet: therefore, many artificial intelligence methods are proposed and evaluated. As one of the methods of processing information from many sensing elements, neural networks (referred to herein as NN) are well known (Wasserman, 1993; Watanabe & Yoneyama, 1992). As for the pattern recognition by vision sensors, there are many researches applying NN for processing image pixel data (Marr, 1982; Sugie, 2000). However, there are few reports applying NN for tactile sensors (Aoyagi et al, 2005; Aoyagi & Tanaka, 2007), since a practical, inexpensive, and widely used tactile sensor composed of many sensing elements has not been established mainly because of fabrication difficulties.

The following of this chapter is constructed as follows:

1. The micromachined force sensing elements under development by the author's group are introduced. One has the silicon structure having a pillar on a diaphragm, on which four piezoresistors are fabricated to detect the distortion caused by a force input to the pillar. Another has the polymer PDMS structure having a concave area inside, on top and bottom surfaces of which aluminum electrodes are deposited, realizing a capacitor.

2. Since a practical arrayed tactile sensor composed of many of the force sensing element is under development, the output of an assumed arrayed type tactile sensor is simulated by the finite element method (FEM). The FEM-simulated stress distribution data are assigned to each assumed stress sensing element of the array. Then, all data of these elements are processed by NN.

3. Imitating the human skin, an arrayed type tactile sensor comprising four layers is proposed and assumed. The information processing method of this sensor is investigated by FEM simulation. A recognizing method of force and its direction is proposed by using two stages NN. A recognizing method of object shape, which is contacted with the sensor surface, is also investigated by a simulation.

2. Example of micromachined force sensing element

2.1 Piezoresistive type

A structure having a pillar and a diaphragm has been developed by authors using micromachining technology. The schematic structure of one sensing element is shown in Fig. 2 (Izutani et al., 2004). Piezoresistors are fabricated on a silicon diaphragm to detect the distortion which is caused by a force input to a pillar on the diaphragm. Three components of force in x, y, and z direction can be simultaneously detected in this sensing element. The principle of measurement is shown in Fig. 3.
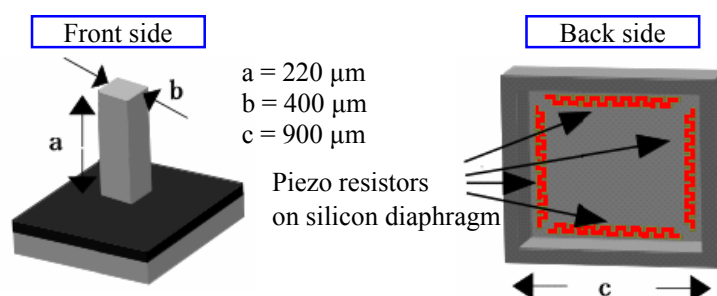

Fig. 2. Schematic structure of sensing element of piezoresistive type

In order to determine the arrangement of piezoresistors, FEM analysis was carried out. The distribution of strain in horizontal direction on the diaphragm when the force of 10 gf is applied vertically to the pillar tip is shown in Fig. 4(a). The distribution when the force is applied horizontally is shown in Fig. 4(b). It is proven that the strain is maximal at the edge of the diaphragm. Therefore, the piezoresistors were arranged near the edge of the diaphragm as far as possible.
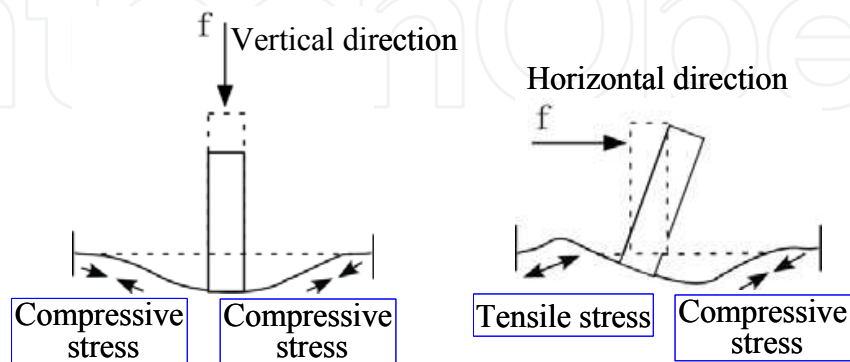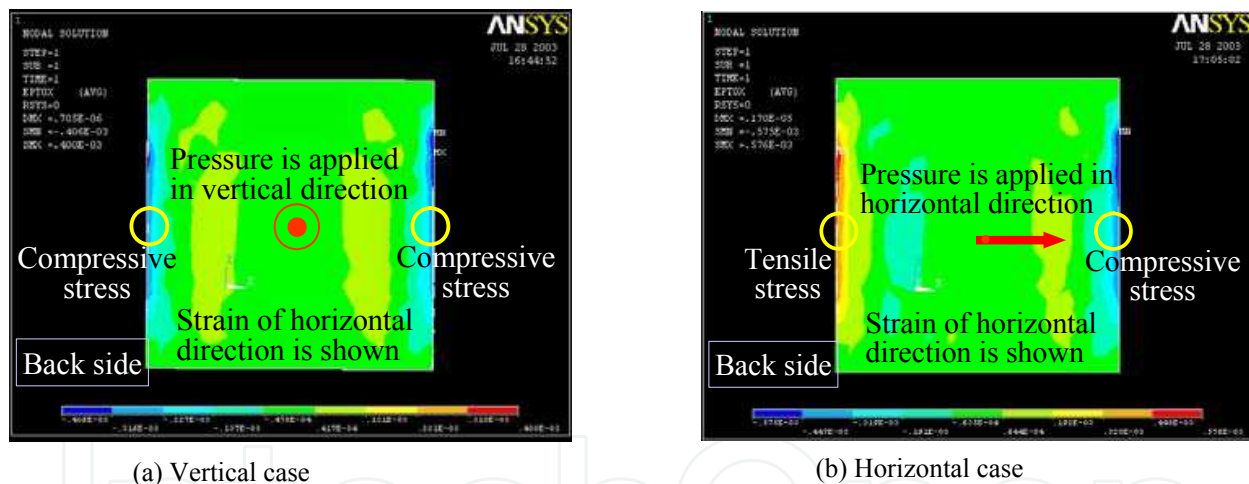

Fig. 3. Principle of force measurement for 3 axes

(a) Vertical case   (b) Horizontal case

Fig. 4. FEM simulation result of distortion of a diaphragm

The micromachining fabrication process of this sensing element is shown in Fig. 5. The SEM image of a fabricated sensing element is shown in Fig. 6. In z direction, it is experimentally proven this element can detect the input force with good linearity within the range from 0 to 200 gf, as shown in Fig. 7. Characterization of performance of force detection in x and y direction, and fabrication of an arrayed type micro tactile sensor by using many sensing elements are ongoing. Furthermore, coating a polymer Parylene (Tai, 2003) film on arrayed elements is planned in future, as shown in Fig. 8. Chemical Vapor Deposition (CVD) can realize a conformal deposition (that is, the deposition is performed not only on the top surface of a target object but also on the back/side surface of it). Four of coated sheets are stacked one by one and bonded to each other, finally forming an arrayed tactile sensor having four layers.

Wet etching of SOI wafer by KOH solution for diaphragm

Boron ion implantation for piezo-resistor, Aluminum patterning for electrode
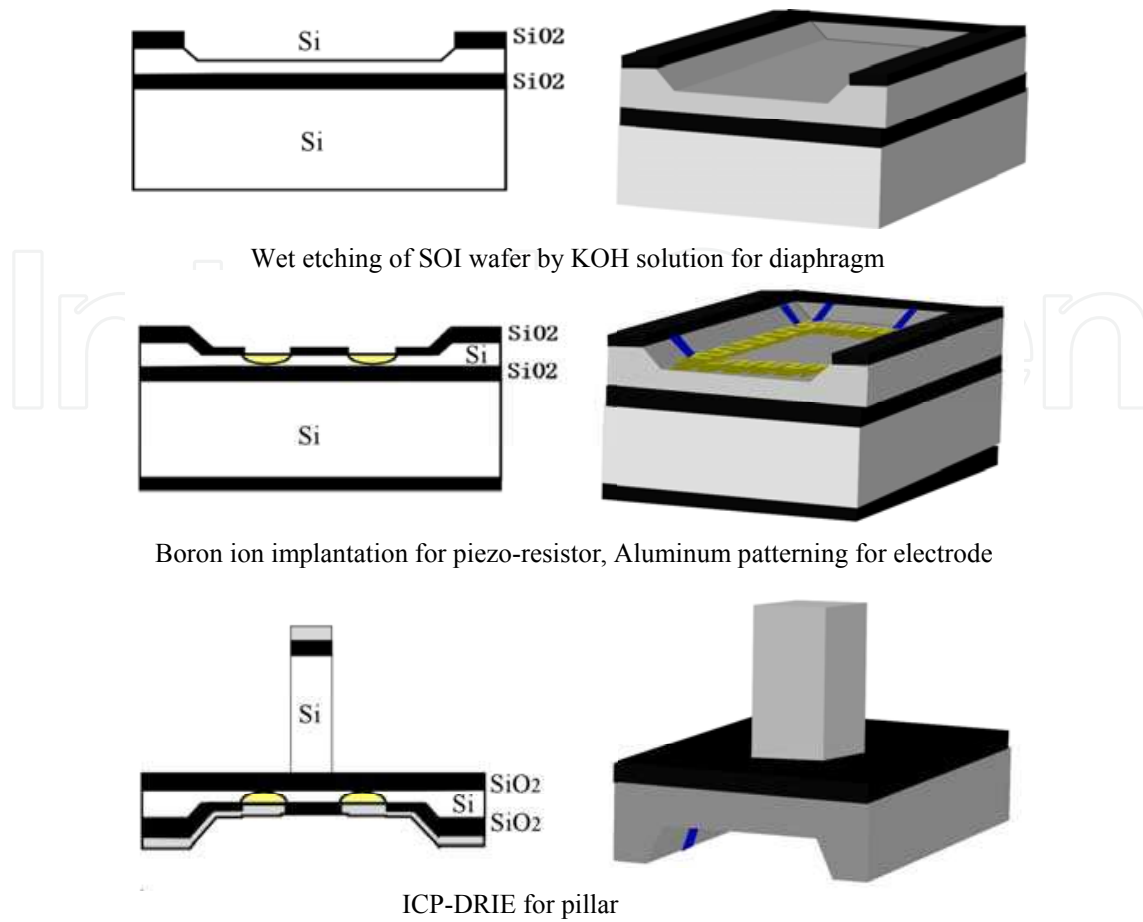

ICP-DRIE for pillar

Fig. 5. Microfabrication process of a force sensing element of Piezoresistive type
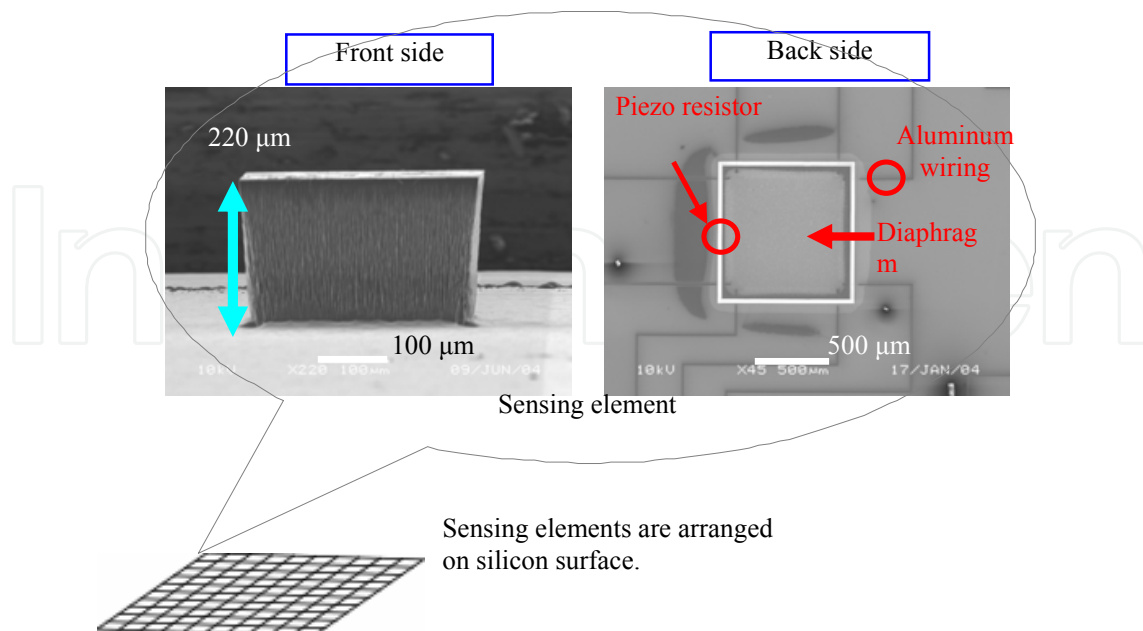

Fig. 6. SEM image of a fabricated sensing element and its application to an array type tactile sensor
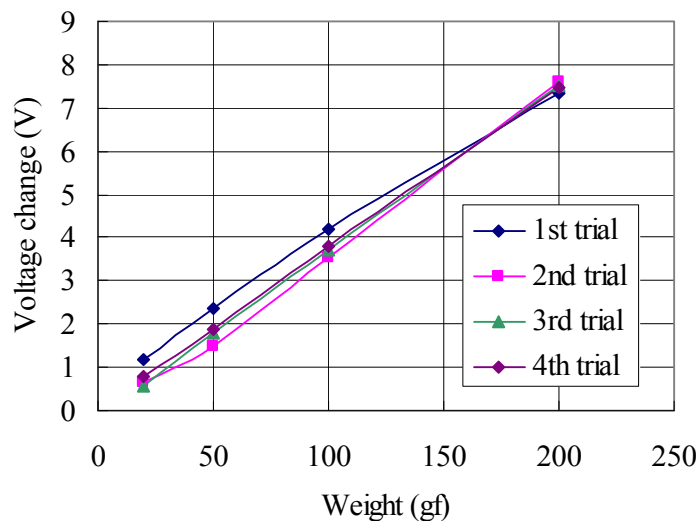
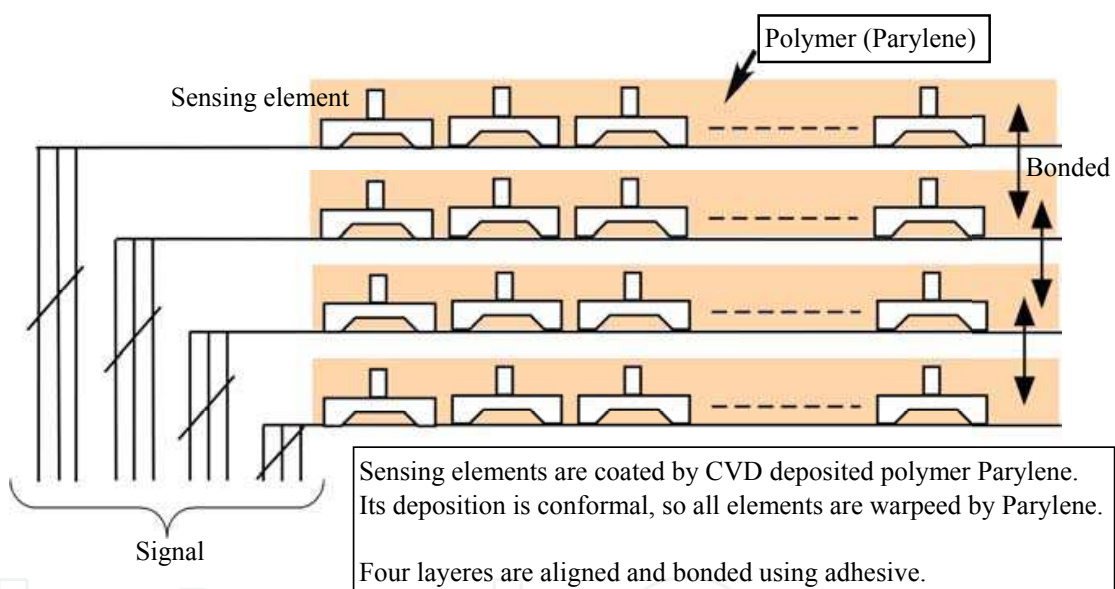Fig. 7. Output voltage change with respect to applied weight

Fig. 8. Four layers tactile sensors comprising polymer sheets deposited on sensing elements (under planning at present)

2.2 Capacitive type

Imitating the human skin structure, a flexible arrayed type tactile sensor having four layers is under development using micromachining technology (Aoyagi & Tanaka, 2007; Ono et al., 2008). The fabrication process of this sensor is shown in Fig. 9. As the material of a layer, polydimethylsiloxane (PDMS), which is a kind of flexible silicone rubber, is used. This process is summarized as follows: one PDMS layer having electrodes is fabricated by a spin-coated method. Another PDMS layer having electrodes is fabricated by a casting method, on which a number of concave space is formed as negative of patterned sacrificial photoresist. These two layers are bonded with each other by applying heat and pressure (see detailed condition in this figure).

Structure with upper

1) Photoresist (OFPR800) is spin-coated on Si substrate for sacrificial layer.
2) Aluminum (1 μm) is deposited and patterned for upper electrodes.
3) PDMS (20-30 μm) is spin-coated as structural material.
4) Photoresist (OFPR800) is spin-coated on Si wafer for the 1st sacrificial layer, followed by hard bake for giving resistivity to O_2 plasma etching afterward.
   Thick photoresit (AZP4903) is spin-coated for the 2nd sacrificial layer (10 μm).
5) Aluminum (1 μm) is deposited and patterned for lower electrodes.
6) The 2nd sacrificial layer is patterned by O_2 plasma.
7) PDMS (300 μm) is cast and cured in air. The 1st and 2nd sacrificial layers are wet etched away using acetone, consequently PDMS structure is pealed off from Si substrate.
8) PDMS structure with lower electrodes is turned over, and bonded to that with upper electrodes under condition as follows: baking temp. is 120℃, pressure is 20 kPa.
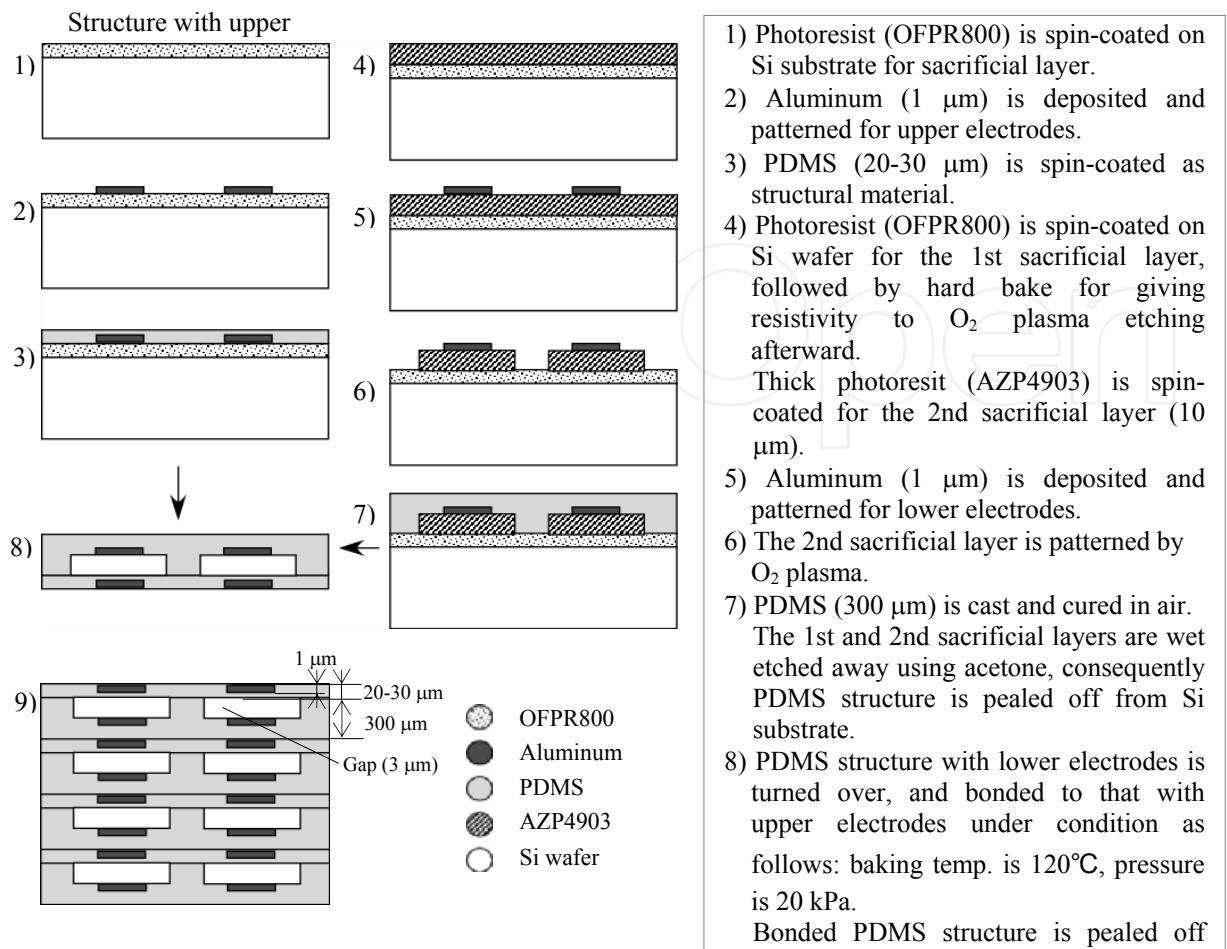   Bonded PDMS structure is pealed off

Fig. 9. Fabrication process of micro tactile sensor composed of many capacitive sensing elements distributed in four PDMS layers

Each sealed concave space has lower and upper electrodes, forming a capacitance. This capacitance changes as the distance between electrodes changes when the structure is deformed based on applied force, i.e., a capacitive force sensing element is realized. The obtained structure having many sensing elements forms one layer, four of which are stacked one by one and bonded to each other, finally forming a tactile sensor having four layers.

A structure of one layer has been fabricated at the moment. An optical image of this structure is shown in Fig. 10(a), of which layout of capacitive sensing elements is shown in Fig. 10(b). Including a 5 by 5 array, many types of arrays are designed on trial. Wiring in one direction, and that in its perpendicular direction are formed, on the crossing areas of which, capacitive sensing elements exist. By selecting corresponding two bonding pads for these two directions, detecting the capacitance of the target sensing element is possible.

The performance of one capacitive force sensing element and that of an arrayed sensor composed of 3×3 elements are characterized. First, a weight was set on the surface of the fabricated sensor having one layer. Then, the capacitance change of one sensing element (1 mm square, 3 μm gap) was detected with the aid of a CV converter IC (MicroSensors Inc., MS3110), the programmable gain of which was set to 0.1 pF/V. Four weights of 5, 10, 20, and 50 gf were employed, of which radii are 5.5, 6.5, 7.5, and 10 mm, respectively. Namely, whole area of one sensing element was covered by each weight and was applied pressure of 516, 738, 1,109, and 1,560 Pa, respectively.
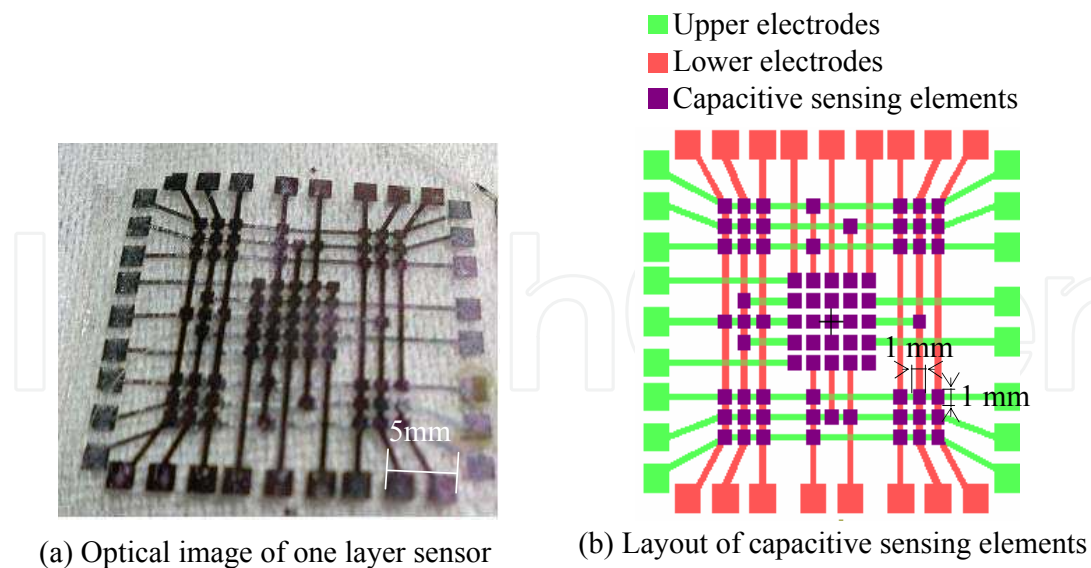
(a) Optical image of one layer sensor   (b) Layout of capacitive sensing elements

Fig. 10. Fabricated sensor having one layer composed of many capacitive sensing elements

(a) 5 gf (516 Pa)   (b) 10 gf (738 Pa)

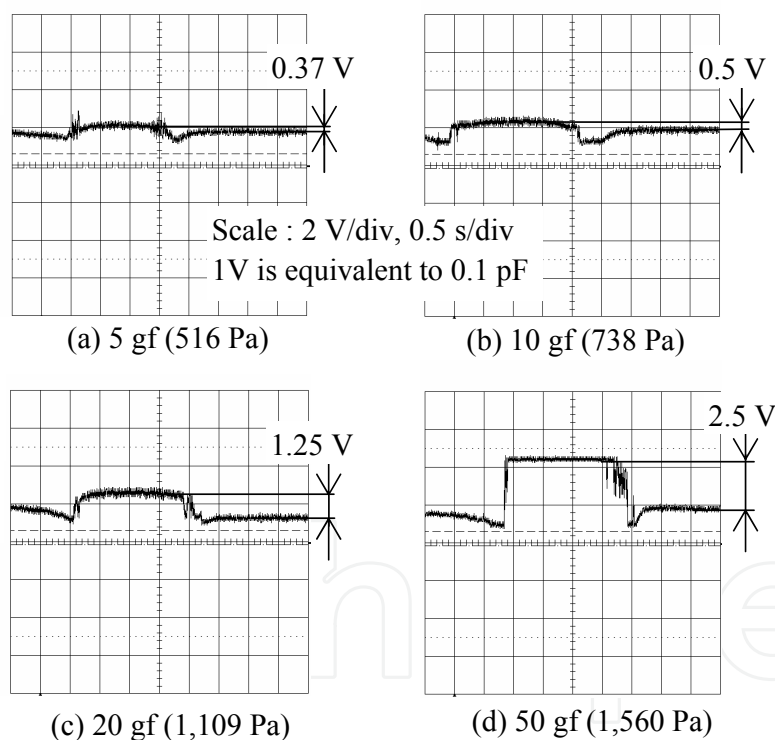(c) 20 gf (1,109 Pa)   (d) 50 gf (1,560 Pa)

Fig. 11. Capacitance change with respect to applied force

Experimental results of output voltage of the IC for several applied force, which are observed by an oscilloscope, are shown in Fig. 11. It is confirmed that the capacitance surely changes by applying force. The results are arranged in Fig. 12, which shows the relationship between the applied pressure and the capacitance change of one sensing element. It is proven that the capacitance increases as the pressure increases. In this figure, the theoretical value is based on the FEM multiphysics simulation, which analyzes the capacitance under

the boundary condition defined by the mechanical deformation of the sensor structure. Measured and theoretical curves have similar trends, although the error is rather large at the pressure of 1,560 Pa.
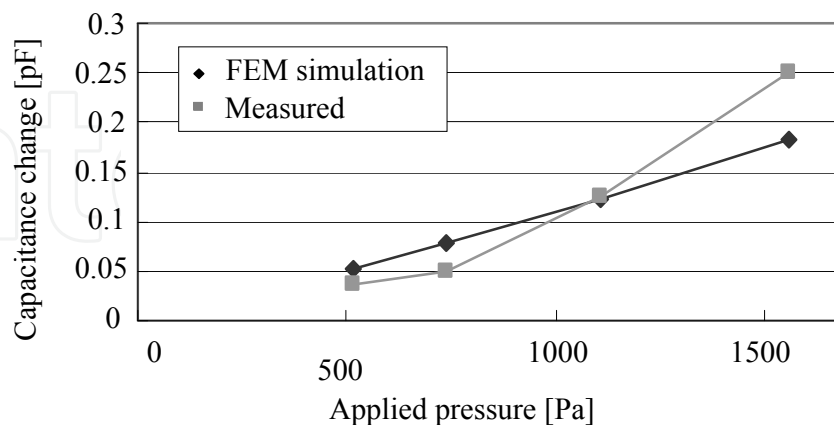

Fig. 12. Relationship between capacitance change and pressure

Next, a distributed load was preliminarily detected using the developed arrayed sensor having one layer. A weight of 5 gf was set, i.e., the pressure of 516 Pa was applied, under two conditions: one is that the weight completely covers the surface area of an arrayed sensor consisting of 3×3 sensing elements (see Fig. 13(a), the sensor exists in the lower right corner of this figure), and another is that the weight partially covers the arrayed sensor, leaving some uncovered elements near the corner of the sensor (see Fig. 13(b)). Then the capacitance change of each sensing element was detected one by one. The results for these cases are shown in Figs. 14(a) and (b), respectively. Looking at these figures, in the former case, almost the constant capacitance changes for all the sensing elements are obtained: while in the latter case, the comparatively lower capacitance changes are obtained at the sensing elements near the corner of the fabricated sensor, where the sensing elements are not covered completely by the weight. These results imply the possibility of this sensor to detect a distributed load.

Weight: 5 gf, Pressure: 516 Pa

(a) A weight completely covers an arrayed sensor.   (b) A weight partially covers an arrayed sensor.

Fig. 13. Experimental condition for distributed load measurement by the arrayed sensor with 3×3 elements
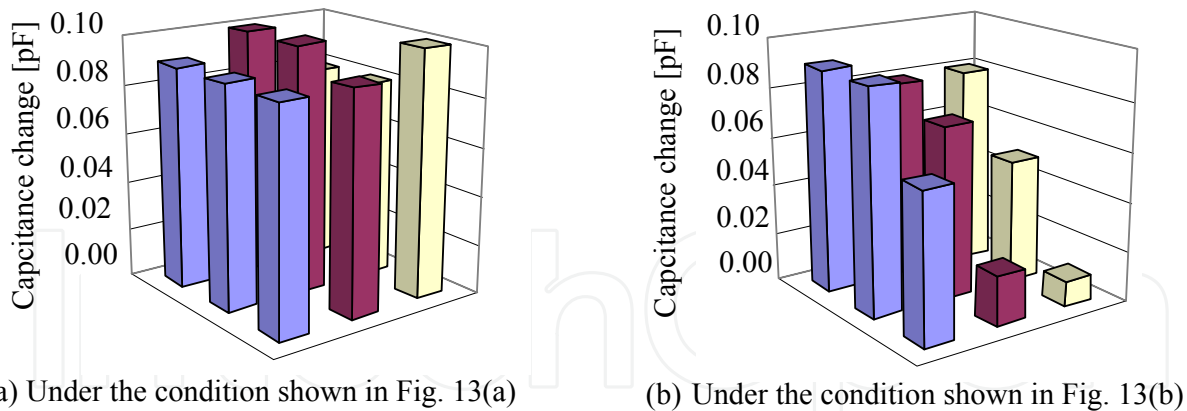
(a) Under the condition shown in Fig. 13(a)   (b) Under the condition shown in Fig. 13(b)

Fig. 14. Result of distributed load measurement

3. FEM simulation on data processing of arrayed tactile sensor having four layers

3.1 Acquisition of contact data by FEM

Since a practical tactile sensor composed of many force sensing elements distributed on four layers is under development, FEM simulation is employed to simulate the data from these sensing elements. As a tactile sensor, an elastic sheet is assumed of which side is 15.0 mm and thickness is 5.0 mm, as shown in Fig. 15. Sensing elements are horizontally distributed in 1.25 mm pitch, and vertically distributed in 1.0 mm pitch. That is, the sensor has four layers, which are positioned at 1 mm, 2mm, 3mm, and 4 mm in depth from the surface. The number of sensing elements is 13×13×4=676 in total. Furthermore, to show the effectiveness of the sensor having four layers, a sensor having one layer is assumed for the reference, of which sensing elements are positioned at 1 mm in depth from the surface, and the number of sensing elements of which is 13×13×1=169 in total.
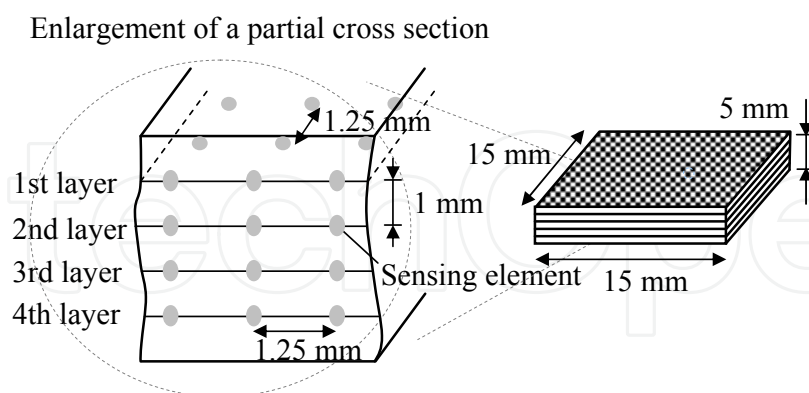

Fig. 15. Assumed model of four layers arrayed type tactile sensor

In case of recognizing force magnitude and its direction using NN (details are explained later in Chapter 4), the stress distribution inside the sensor sheet is simulated under the condition shown in Fig. 16. ANSYS (ANSYS, Inc.) is used as simulation software. As a material of composition, PDMS (Young's modulus: 3.0 MPa) is assumed. Distributed load is applied to the circle of 3 mm in radius on the sheet surface. An object that cuts diagonally a

cylinder is used to apply the force, because this software is difficult to deal with a diagonal load to a sheet surface. The friction of coefficient between the sheet surface and the bottom of object is assumed to be 1.0. Under this condition, stress distribution inside the sheet is simulated for many times, changing the force magnitude and its direction. Considering the sensing range of the practical arrayed tactile sensor under development, the applied force magnitude is changed within the range from 10 to 200 gf. Figure 17 shows a simulated example of distribution of Mises stress σ_{mises}, when θ is 15º and force is 10 gf.
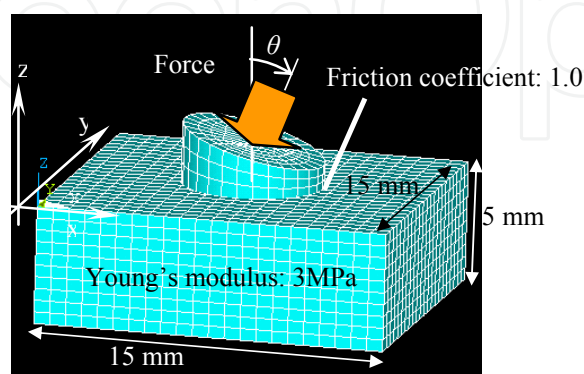

Fig. 16. FEM simulation condition of stress distribution for contact force recognition
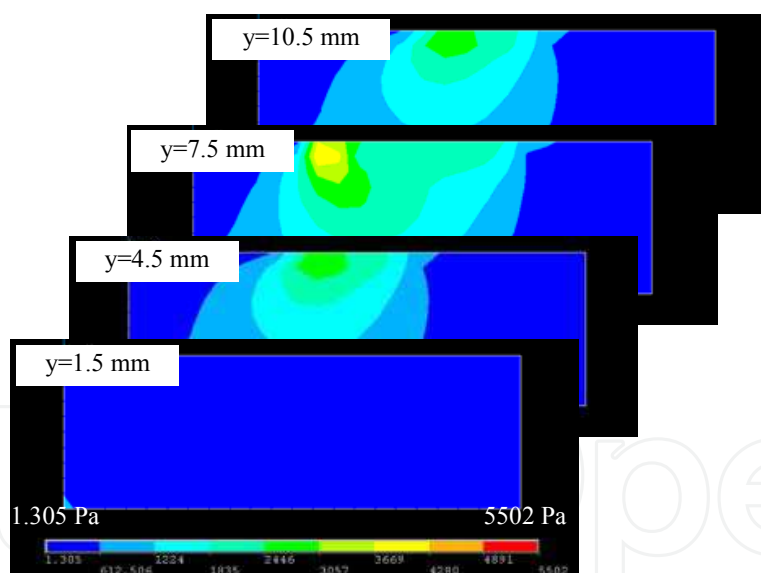

Fig. 17. FEM simulation result of stress distribution for contact force recognition (in case of θ=15 degree)

In case of recognizing the shape of contact object using NN (details are explained later in Chapter 5), the stress distribution in the sensor sheet is simulated under the condition shown in Fig. 18 (a). The contact objects having various bottom shapes are employed. Each object is pressed vertically, i.e., under θ =0º, against the assumed tactile sensor, being applied force of which magnitude is 10 gf. Figure 18(b) shows a simulated example of distribution of σ_{mises}, where the bottom shape of object is circle.

10gf is applied vertically.
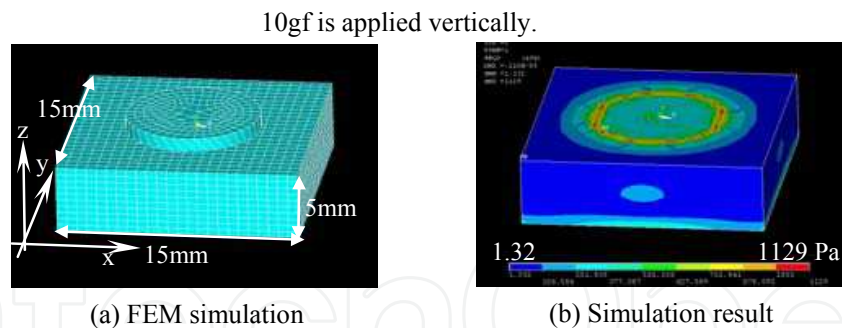

| (a) FEM simulation | (b) Simulation result |

Fig. 18. FEM simulation of stress distribution for object shape recognition (in case of circle shape)

3.2 Assignment of FEM data to sensing elements

It is necessary to assign σ_{mises} at each node on FEM meshed element to each sensing element of the tactile sensor (Fig. 15). A sampling area of 0.625 mm in radius, of which center is the position of a sensing element, is assumed. The σ_{mises} data of FEM nodes within this area are averaged, being assigned to the corresponding sensing element as its output.

4. Recognition of contact force

4.1 Recognition method of force magnitude and its direction using two stages neural networks

In usual NN researches, several features, such as area, surrounding length, color, etc., are extracted from raw data, and they are input to NN. On the other hand, in this research, all raw data are directly input to NN at the first step, considering that the information processing mechanism in the human brain has not been cleared, i.e., whether some features are extracted or not, and what features are extracted if so.

In usual researches, single NN is used for pattern recognition. In case of tactile sensing, single NN may be possible, to which stress data of sensing elements are input, and from which three components f_x, f_y, f_z of force vector are output. However, in case of recognizing both magnitude and its direction with practical high precision by single NN, numerous training data and long training time would be necessary. On the other hand, in this case, as far as the force direction is kept to be identical, the aspect of stress distribution does not change, whereas the stress value at each sensing element changes linearly in proportion to the input force magnitude. Therefore, force direction could be detected irrespective of force magnitude by normalizing stress data of all sensing elements from 0 to 1, and inputting them to the first stage NN (Fig. 19). Then, the direction information, i.e., three components of the normalized unit force vector, and the maximum stress value of each layer, are input to the second stage NN for detecting the force magnitude (Fig. 20). Since NN of each stage perform its own allotted recognition processing, the number of training data and training time are expected to be much reduced, keeping high detecting precision.

As a learning method of network's internal state that decreases the error between NN outputs and training data, RPROP method (Riedmiller & Braun, 1993) modifying the well-known back propagation method is adopted. Stress distribution data of unknown force vectors are input to the learned two stages NN, and its direction and magnitude are recognized. From these results, the generalization ability of the NN is investigated.
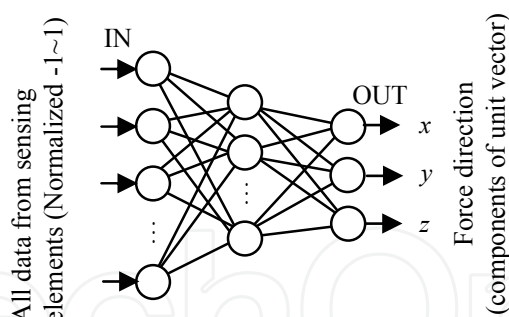
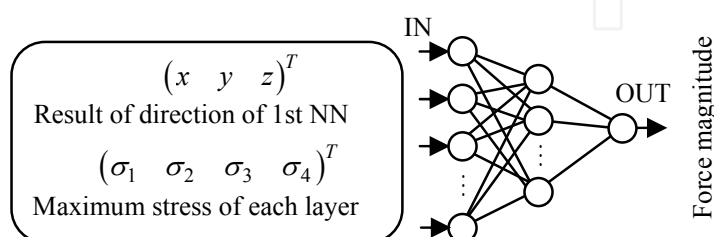Fig. 19. First stage neural networks for force direction recognition

Fig. 20. Second stage neural networks for force magnitude recognition

4.2 Results of force direction recognition

The number of neurons of the first stage NN (see Fig. 19) is as follows: 676 for input group in case of the four layers sensor (this is 169 in case of the one layer sensor), 20 for hidden group, and 3 for output group. Stress information of all the sensing elements is input to the neurons of input group. The neurons of output group determine the unit vector of applied force (3 outputs). Training data are 8 kinds of stress distribution, of which force direction θ (see the definition of θ in Fig. 16) ranges from 0 to 35° in 5° intervals. The convergence of learning of NN is good for both of the one layer sensor and the four layers sensor, of which training error is equivalent to 0.04°, as shown in the second line of Table 2.

As the unknown test data, four kinds of stress distribution, of which force directions θ are 1, 13, 18, and 27°, are input to the learned NN. The output of NN is converted to θ, which is shown in Table 2. It is proven that the recognition accuracy of the four layers sensor is slightly better than that of the one layer sensor. The errors are within 0.2° for both cases.

	NN of one layer sensor	NN of four layers sensor
Training error	0.04°	0.04°
Unknown input 1°	0.8°	0.9°
Unknown input 13°	12.8°	13.0°
Unknown input 18°	18.0°	18.0°
Unknown input 27°	26.8°	27.2°

Table 2. Results of force direction recognition

4.3 Results of force magnitude recognition

The number of neurons of the second stage NN (see Fig. 20) is as follows: 7 for input group in case of the four layers sensor (this is 4 in case of the one layer sensor), 169 for hidden group, and 1 for output. The output of NN is from 0 to 1, normalizing the full range of sensor output, which is from 0 to 200 gf. Training data are 160 kinds of stress distribution,

i.e., 8 kinds of degree ranging from 0 to 35º in 5º intervals, 20 kinds of force magnitude ranging from 0 to 200 gf in 10 gf intervals, then 8×20=160 kinds in total. Contrary to the case of force direction recognition, the convergence of learning the NN is not so good, depending on initial connection weights of neurons. Therefore, ten kinds of initial connection weights are tested, from which the NN is learned, setting the limit of iteration number to 100,000. Obtained training errors for them are averaged, and described in the second line of Table 3, showing that the training error for the one layer sensor is inferior to that for the four layers sensor.

One NN realizing the smallest training error is selected among the ten, the generalization ability of which is estimated. As the unknown test data, 76 kinds of stress distribution are prepared, of which θ and force magnitude are as follows: θ are 1, 13, 18, and 27º, and force magnitudes are from 15 to 195 gf in 10 gf interval. The outputs of the NN for the test data are evaluated by comparing them with true values of force magnitude. The results of absolute errors between them in case of the one layer sensor are shown in Fig. 21. Those in case of the four layers sensor are shown in Fig. 22. The average and the standard deviation of all the absolute errors are calculated for each case, which are shown in the third and forth lines of Table 3.

From these results, it is proven that the accuracy of force magnitude recognition of the four layers sensor is fairly better than that of the one layer sensor. The reason of this advantage of the four layers sensor compared to the one layer sensor would be based on its larger number of sensing elements distributed not only horizontally but also vertically, realizing a fine interpolation of nonlinear characteristics of stress distribution caused by applied force, which does not contradict the better convergence of learning NN (see the second line of Table 3).

	NN of one layer sensor	NN of four layers sensor
Average of training error	0.003 [gf]	0.001 [gf]
Absolute average error	0.53 [gf]	0.23 [gf]
Standard deviation	0.17 [gf]	0.03 [gf]

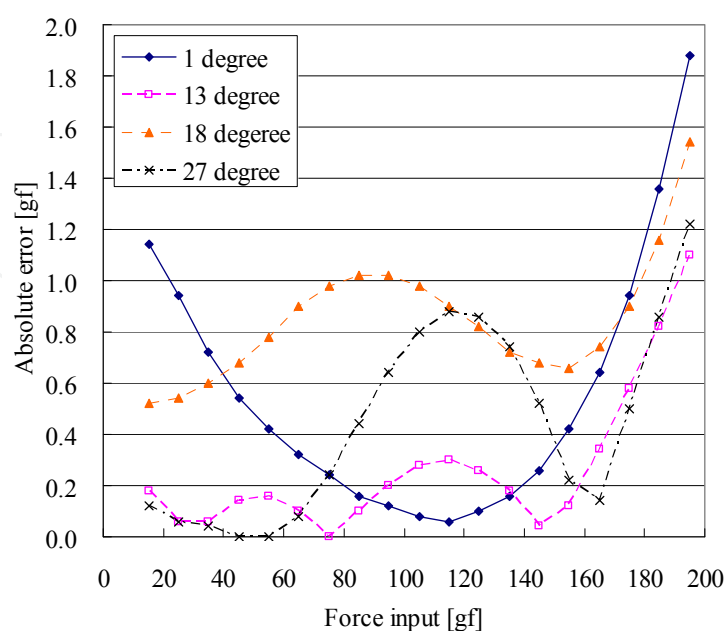Table 3. Results of force magnitude recognition

Fig. 21. Absolute errors between NN outputs and true values (in case of one layer sensor)
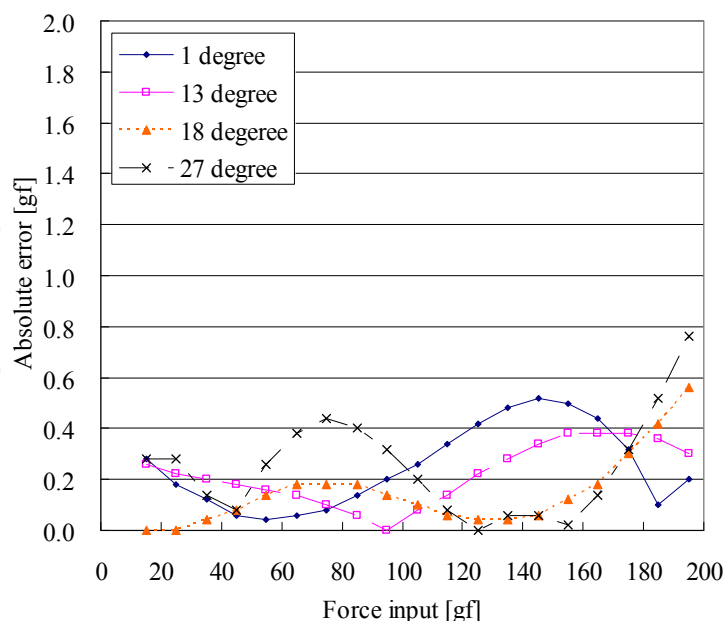
Fig. 22. Absolute errors between NN outputs and true values (in case of four layers sensor)

5. Recognition of object shape

5.1 Recognition method of object shape using neural networks

The shape of contact object is recognized by applying NN to the FEM simulated data of force sensing elements. It is assumed that only approximate contact position is known by some recognition method. Then, the important point is to recognize the shape with robustness to unwanted shift of the object from the reference position, where the template for the recognition was constructed. The method using NN for object shape recognition is schematically shown in Fig. 23.
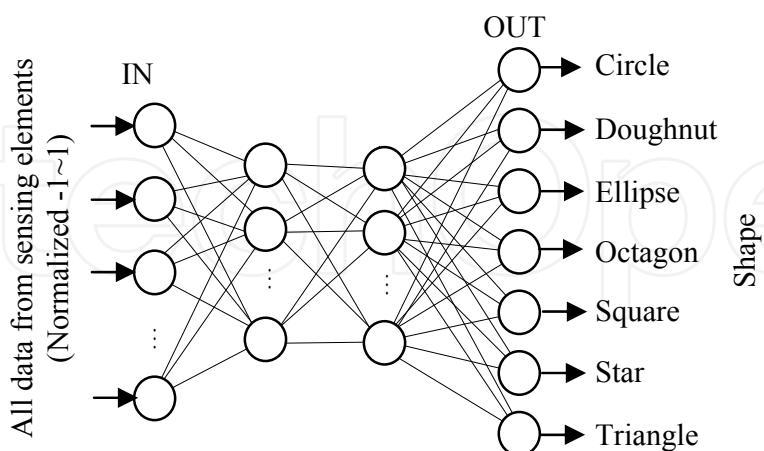

Fig. 23. Neural networks for object shape recognition

As the object shape, seven kinds of circle, doughnut, ellipse, octagon, square, star, and triangle are employed, which are circumscribed for a 10 mm square. As the training data, the stress distributions are simulated by FEM, when the objects are positioned precisely in

the center of the sensor surface of 15 mm square, and pressed vertically by applying 10 gf force. As a learning method of network's internal state, RPROP method (explained in Section 4.1) is adopted.

The unknown test data are prepared, which are obtained from the stress distributions when the objects are shifted from the center of the sensor surface by 1.25 mm. This shift is beyond 10% of the object side, which is comparatively large. Using these data, the generalization ability of NN is investigated, and the effectiveness of using four layers is estimated.

5.2 Results of object shape recognition

The number of neurons of the NN (see Fig. 23) in case of the four layers sensor is as follows: 676 for input group, 676 for the first hidden group, 20 for the second hidden group, and 7 for output group. That in case of the one layer sensor is as follows: 169 for input group, 169 for the first hidden group, 13 for the second hidden group, and 7 for output group. The employment of two hidden groups, and the definition of the number of neurons of them are based on the adjustment by trial and error. Note that the adjustment in case of the four layers sensor was much easier than that in case of the one layer sensor, implying the good interpolating ability of using four layers.

The results of object shape recognition for unknown objects are shown in Table 4 and Fig. 24(a) in case of the one layer sensor. Those in case of the four layers sensor are shown in Table 5 and Fig. 24(b). The shaded values in these tables are the maximum NN's output value among the seven candidates. Seeing Table 4, in case of the one layer sensor, the circle is mistaken for the ellipse, whereas the doughnut and the octagon are mistaken for the circle. By contrast, seeing Table 5, all objects are finely recognized as the correct shapes in the case of the four layers sensor.

Unknown input	Output of NN in case of the one story sensor						
	Circle	Doughnut	Ellipse	Octagon	Square	Star	Triangle
Circle	0.62	0.00	0.99	0.00	0.00	0.00	0.00
Doughnut	0.89	0.00	0.00	0.00	0.00	0.00	0.00
Ellipse	0.00	0.00	1.00	0.00	0.00	0.00	0.00
Octagon	0.62	0.00	0.38	0.13	0.00	0.00	0.00
Square	0.00	0.00	0.00	0.00	0.97	0.00	0.00
Star	0.00	0.00	0.00	0.16	0.00	0.98	0.00
Triangle	0.00	0.00	0.00	0.00	0.00	0.00	1.00

Table 4. Results of object shape recognition by NN in case of the one layer tactile sensor

Unknown input	Output of NN in case of the four stories sensor						
	Circle	Doughnut	Ellipse	Octagon	Square	Star	Triangle
Circle	0.95	0.00	0.00	0.00	0.01	0.00	0.00
Doughnut	0.00	0.99	0.00	0.00	0.00	0.00	0.00
Ellipse	0.00	0.00	1.00	0.00	0.01	0.00	0.00
Octagon	0.01	0.00	0.00	0.81	0.00	0.00	0.00
Square	0.00	0.00	0.01	0.00	1.00	0.00	0.00
Star	0.00	0.00	0.00	0.00	0.00	0.99	0.00
Triangle	0.00	0.00	0.00	0.00	0.00	0.01	1.00

Unknown objects shifted from the center of sensor by 1.25 mm are recognized.

Table 5. Results of object shape recognition by NN in case of the four layers tactile sensor

(a) In case of the one layer tactile sensor   (b) In case of the four layers tactile sensor
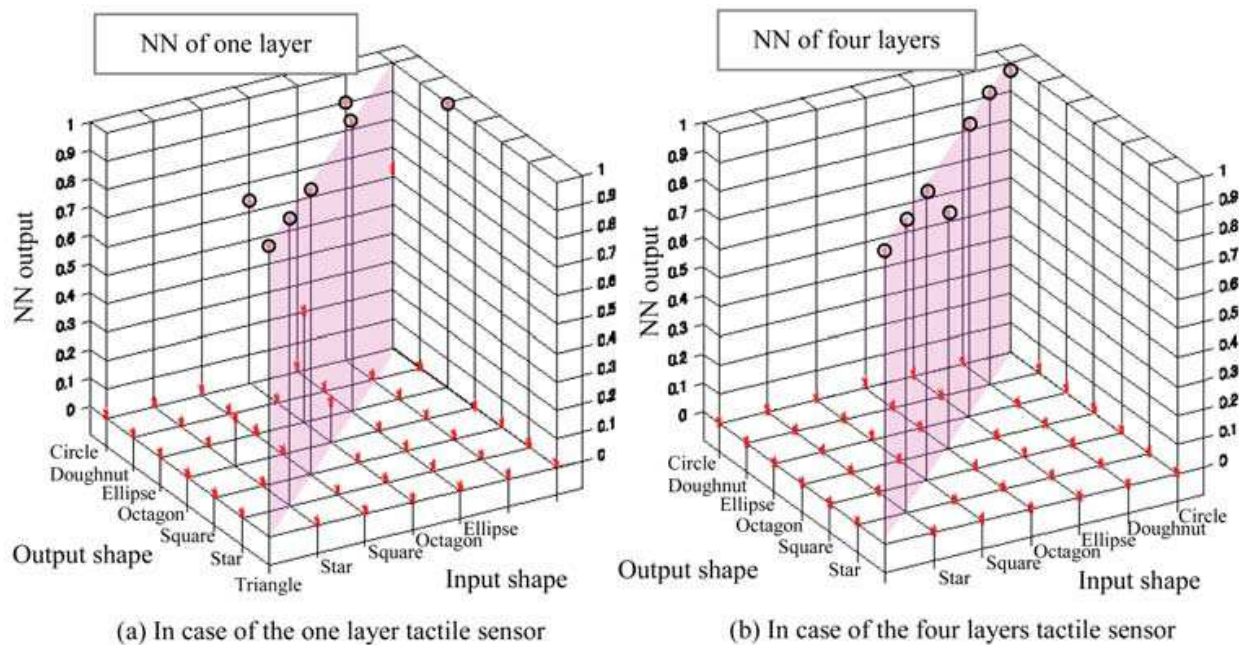
Fig. 24. NN output of tactile sensor for unknown object shape

The stress distributions on each surface of the four layers are shown in Fig. 25. Seeing this figure, the contour edge of stress distribution becomes obscure as the depth becomes large, which means the influence of the object shift on the stress distribution change becomes smaller. If four layers are employed, the stress information of deeper layers, which is robust to the object shift, is available, which would be one of the reasons for the higher recognition ability of using four layers compared to that of using only one layer.
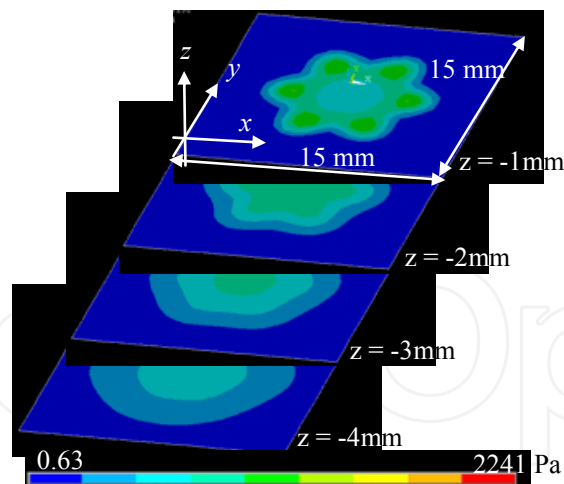

Fig. 25. Stress distribution on each surface of the four stories (in case of star shape)

6. Comparison with human tactile sensing

The density of tactile receptors in the human finger is very high and some optimum information processing may be carried out in the human brain. To compare the ability of artificial NN with that of a human being, the experiment is carried out in which a human senses object shape by finger touch, while his eye is occluded by a bandage. The situation of

this experiment is shown in Fig. 26. Three subjects of circle, triangle, and square are adopted. Two human testers are employed. Each of them touches randomly 30 subjects. The result is shown in Table 6. Also, NN simulation is applied to this case, and the result is shown in the same table.

Fig. 26. Situation of object shape recognition by human being

	Circle	Triangle	Square
Human（testers A and B）	100.0%	100.0%	100.0%
Neural networks	96.8%	100.0%	98.2%

Table 6. Comparison between human and neural networks

Seeing this result, human ability is fairly good, whereas NN ability is a little bit inferior to human ability, but not so bad. The mechanism of tactile sensing of human being is not clear; however, NN is a good candidate imitating human tactile ability, and authors think improving the recognition rate of NN is possible by increasing the number of sensing elements and selecting appropriate parameters of NN, such as the number of neurons, the number of hidden groups, etc.

7. Module networks for detecting total contact state

On the basis of this research, constructing networks (not restricted to neural networks) which can recognize not only force direction/magnitude and object shape but also size, contact position, orientation, texture, etc., totally is a projected work. The authors are planning to use module type networks, of which concept is schematically shown in Fig. 27. In this type networks, for example, if an object of different shape is added, the system can cope with this case only by re-learning a network for object shape recognition (not re-learning all networks), which reduces training data number and learning time. Modulation makes it possible to select effective and proper recognition methods not limited to NN, such as Support Vector Machine (SVM) (Cristianini & Taylor, 2000) etc., which would improve the recognition ability of the whole system.

In our previous research (Aoyagi et al., 2005), single NN recognize the object shape contacted with a sensor sheet despite size and contact position: however, enormous training data of stress distribution changing size and contact position variously were needed. As for this single NN, in order to cope with adding kinds of recognized objects, the learning process must be carried out again from the start, which needs more training data and training time as far as keeping a practical recognition rate. To solve this problem, in the projected work, two network modules which determine size and contact position respectively are used (Fig. 27). From the output of these two modules, the most suitable NN

is selected to recognize the object shape. By using the modulation method described here, reducing training data number, increasing recognition rate, increasing generalization ability, etc., are expected in future.
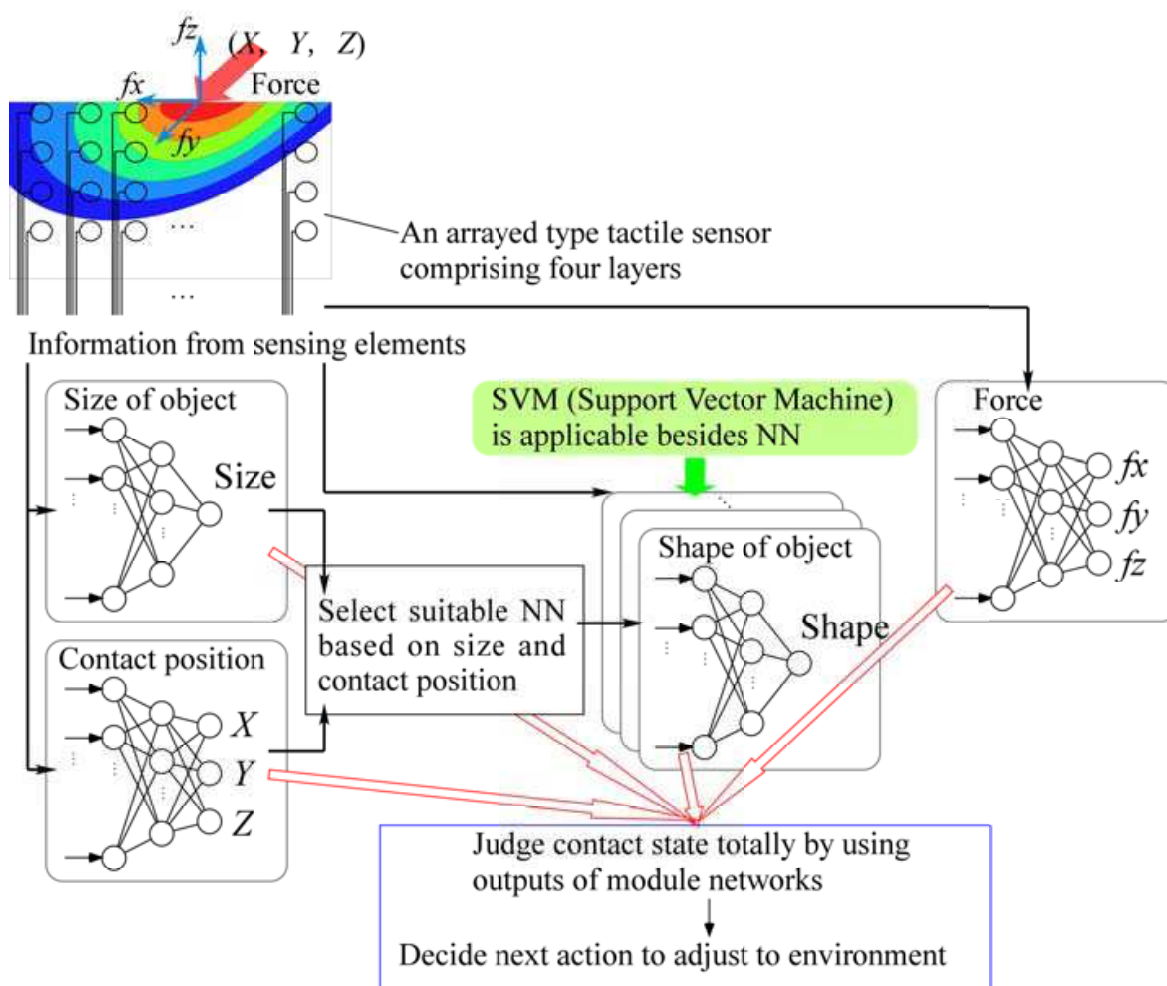

Fig. 27. Concept of module networks for detecting total contact state

8. Conclusions

A tactile sensor having four layers is proposed, and the information processing method for this sensor using neural networks (NN) is investigated. The summary is as follows: 1) Imitating the human skin structure, an arrayed type tactile sensor composed of many force sensing elements distributed on four layers is proposed. 2) The micromachining process for the four layers sensor composed of many capacitive sensing elements is proposed. 3) The output data from the force sensing elements are simulated by FEM. 4) For recognizing the contact force, two stages NN, the first stage of which is for detecting force direction and the second stage of which is for detecting force magnitude, is proposed. The effectiveness of this method is confirmed by simulation. 5) The contact object shape is recognized by simulation, confirming the effectiveness of NN. 6) In both cases of force recognition and shape recognition, the sensor having four layers is confirmed to be superior to that having one layer, in the viewpoint of recognition accuracy. 7) A concept of module networks for detecting total contact state is proposed.

The novelties of this study on tactile sensor are 1) using four layers, 2) using raw data of all sensing elements and inputting them to NN, and 3) proposing two stages NN and module networks.

9. Acknowledgments

10. References

Aoyagi, S.; Tanaka, T. & Makihira, K. (2005). Recognition of Contact State by Using Neural Network for Micromachined Array Type Tactile Sensor. *Int. J. Information Acquisition*, Vol. 2, No. 3, pp. 1-10

Aoyagi, S. & Tanaka, T. (2007). Proposal of a Micromachined Tactile Sensor Having Four Stories and Its Information Processing Method Using Module Networks. *Neural Information Processing –Letters and Reviews*, Vol. 11, Nos. 4-6, pp. 147-158

Cristianini, N. & Taylor, J. S. (2000). *An Introduction to Support Vector Machines and Other Kernel-Based Learning Methods*, Cambridge University Press, ISBN 0-521-7809-5, Cambridge, UK

Esashi, M.; Shoji, S.; Yamamoto, A. & Nakamura, K. (1990). Fabrication of Semiconductor Tactile Imager. *Trans. Institute Electronics, Information and Communication Engineers*, Vol. J73-C-II, No. 1, pp. 31-37

Hiraishi, H.; Suzuki, N.; Kaneko, M. & Tanie, K. (1989). Profile Detection of Objects by a High-Resolution Tactile Sensor Using a Light Conductive Plate. *J. Japan Society of Mechanical Engineers*, Vol. 55, No. 516, pp. 2091-2099 (in Japanese)

Horie, M.; Funabashi, H. & Ozawa, T. (1995). Development of Three-Axial Force Sensors for Microrobots. *J. Japan Society of Mechanical Engineers*, Vol. 61, No. 591, pp. 4563-4568 (in Japanese)

Ishikawa, M. & Shimojjo, M. (1988). An Imaging Tactile Sensor with Video Output and Tactile Image Processing. *J. Society of Instrument and Control Engineers*, Vol. 24, No. 7, pp, 662-669

Izutani, J.; Maeda, Y. & Aoyagi, S. (2004). Development of a Micro Tactile Sensor utilizing Piezoresistors and Characterization of its Performance. *Proc. International Conference on Machine Automation (ICMA2004)*, pp. 193-196, Osaka, Japan, November 2004

Kamiyama, K.; Kajimoto, H.; Inami, M.; Kawakami, N. & Tachi, S. (2003). Development of A Vision-based Tactile Sensor. *Trans. Institute of Electrical Engineers of Japan*, Vol. 123, No. 1, pp. 16-22 (in Japanese)

Kane, B. J.; Cutkosky, M. R. & Kovacs, G. A. (2000). A Tactile Stress Sensor Array for Use in High-Resolution Robotic Tactile Imaging. *J. Microelectromechanical Systems*, Vol. 9, No. 4, pp. 425-434

Kinoshita, G. (1981). Overview of the Basic Research needed to advance the Robotic Tactile Sensors. *J. The Robotics Society of Japan*, Vol. 2, No. 5, pp. 430-437 (in Japanese)

Kobayashi, M. & Sagisawa, S. (1991). Three Direction Sensing Silicon Tactile Sensors. *Trans. Institute Electronics, Information and Communication Engineers*, Vol. J74-C-II, No. 5, pp. 427-433

Kovacs, G. T. A. (1998). *Micromachined Transducers Sourcebook*, McGraw-Hill, ISBN 0-07-290722-3, New York, USA

Lee, M. H. & Nicholls, H. R. (1999). Tactile Sensing for Mechatronics -A State of the Art Survey-. *Mechatronics*, Vol. 9, pp. 1-31

Lee, H. K.; Chang, S. I. & Yoon, E. (2006). A Flexible Polymer Tactile Sensor: Fabrication and Modular Expandability for Large Area Deployment. *J. Microelectromechanical Systems*, Vol. 15, No. 6, pp. 1681-1686

Maeda, Y.; Aoyagi, S.; Takano, M. & Hashiguchi, G. (2004). Development of a Micro Tactile Sensor for Robot Application and Its Evaluation. *Proc. Spring Meeting of Japan Society for Precision Engineering*, pp. 1121-1122, Tokyo, Japan, March 2004 (in Japanese)

Maekawa, H.; Tanie, K.; Kaneko, M.; Suzuki, N.; Horiguchi, C. & Sugawara, T. (1994). Development of a Finger-Shaped Tactile Sensor Using a Hemispherical Optical Waveguide. *J. Society of Instrument and Control Engineers*, Vol. 30, No. 5, pp. 499-508

Maeno, T. (2000). Structure and Function of Finger Pad and Tactile Receptors. *J. The Robotics Society of Japan*, Vol. 18, No. 6, pp. 767-771 (in Japanese)

Marr, D. (1982). *Vision: A Computational Investigation into the Human Representation and Processing of Visual Information*. Freeman, W. H. and Company, ISBN 0716712849, New York, USA

Matsushita, T.; Aoyagi, S. & Kozuka, H. (2004). Sol-gel Preparation of a PZT Thick Film from a Solution Containing Polyvinylpyrrolidone and Its Application for a Micro Ultrasonic Sensor. *Proc. Asia-Pacific Conf. Transducers and Micro-Nano Technology 2004 (APCOT2004)*, pp. 159-162, Sapporo, Japan, July 2004

Nguyen, A. T.; Dao, D. V.; Toriyama, T.; Wells, J. C. & Sugiyama, S. (2004). Measurement of Loads Acting on a Near-Wall Particle in Turbulent Water Flow by Using a 6-DOF MEMS-Based Sensor. *Proc. Asia-Pacific Conf. Transducers and Micro-Nano Technology (APCOT2004)*, pp. 508-512, Sapporo, Japan, July 2004

Ohka, M.; Kobayashi, M.; Shinokura, T. & Sagisawa, S. (1990). Data Processing of Tactile Information for Three-Axis Tactile Sensor. *J. Japan Society of Mechanical Engineers*, Vol. 56, No. 531, pp. 2919-2925 (in Japanese)

Ono, D.; Fukutani, T. & Aoyagi, S. (2008). Development of an Arrayed Tactile Sensor Having Four Stories and Recognition of Contact Using Neural Networks, *IEEJ Transaction SM*, Vol. 128, No. 5, pp. 246-251

Riedmiller, M. & Braun, H. (1993). A Direct Adaptive Method for Faster Backpropagation Learning: The RPROP Algorithm. *Proc. IEEE International Conference on Neural Networks*, pp. 586-591, San Francisco, USA, March 1993.

Shinoda, H. (2000). Tactile Sensing for Dexterous Hand. *J. The Robotics Society of Japan*, Vol. 18, No. 6, pp. 772-775 (in Japanese)

Sugie, N. (2000). Sensory Information Processing by Means of Neuro-computing. *J. The Robotics Society of Japan*, Vol. 9, No. 2, pp. 209-216 (in Japanese)

Suzuki, K.; Najafi, K. & Wise, K. D. (1990). A 1024-Element High-Performance Silicon Tactile Imager. *IEEE Trans. Electron Devices*, Vol. 37, No. 8, pp.1852-1860

Tai, Y. C. (2003). Parylene MEMS: Material, Technology and Application. *Proc. 20th Sensor Symp.*, pp. 1-8, Tokyo, Japan, July 2003

Takao, H.; Sawada, K. & Ishida, M. (2005). Multifunctional Smart Tactile-Image Sensor with Integrated Arrays of Strain and Temperature Sensors on Single Air-Pressurized Silicon Diaphragm. *Tech. Digest Transducers '05*, pp. 45-48, Seoul, Korea, June 2005

Wasserman, P. D. (1993). *Advanced Methods in Neural Computing*, Van Nostrand Reinhold, ISBN 0442004613, New York, USA

Watanabe, S. & Yoneyama, M. (1992). An Ultrasonic Visual Sensor for Three-Dimensional Object Recognition Using Neural Networks, *IEEE Trans. Robotics and Automation*, Vol. 8, No. 2, pp. 240-249

Yagi, S. (1991). Array Tactile Sensor using Piezoelectric Film. *J. The Robotics Society of Japan*, Vol. 7, No. 7, pp. 906-907 (in Japanese)

Sensors: Focus on Tactile Force and Stress Sensors

Edited by Jose Gerardo Rocha and Senentxu Lanceros-Mendez

This book describes some devices that are commonly identified as tactile or force sensors. This is achieved with different degrees of detail, in a unique and actual resource, through the description of different approaches to this type of sensors. Understanding the design and the working principles of the sensors described here requires a multidisciplinary background of electrical engineering, mechanical engineering, physics, biology, etc. An attempt has been made to place side by side the most pertinent information in order to reach a more productive reading not only for professionals dedicated to the design of tactile sensors, but also for all other sensor users, as for example, in the field of robotics. The latest technologies presented in this book are more focused on information readout and processing: as new materials, micro and sub-micro sensors are available, wireless transmission and processing of the sensorial information, as well as some innovative methodologies for obtaining and interpreting tactile information are also strongly evolving.

How to reference

In order to correctly reference this scholarly work, feel free to copy and paste the following:

Seiji Aoyagi (2008). Recognition of Contact State of Four Layers Arrayed Type Tactile Sensor by Using Neural Networks, Sensors: Focus on Tactile Force and Stress Sensors, Jose Gerardo Rocha and Senentxu Lanceros-Mendez (Ed.), ISBN: 978-953-7619-31-2, InTech, Available from:
http://www.intechopen.com/books/sensors-focus-on-tactile-force-and-stress-sensors/recognition_of_contact_state_of_four_layers_arrayed_type_tactile_sensor_by_using_neural_networks

INTECH
open science | open minds